ADVANCED FUNCTIONAL MATERIALS

Mechanical Gradient Cues for Guided Cell Motility and Control of Cell Behavior on Uniform Substrates

By *Barbara Cortese,* Giuseppe Gigli,* and *Mathis Riehle*

A novel method for the fabrication and the use of simple uniform poly(dimethylsiloxane) PDMS substrates for controlling cell motility by a mechanical gradient is reported. The substrate is fabricated in PDMS using soft lithography and consists of a soft membrane suspended on top of a patterned PDMS substrate. The difference in the gradient stiffness is related to the underlying pattern. It is shown experimentally that these uniform substrates can modulate the response of cell motility, thus enabling patterning on the surfaces with precise cell motility. Because of the uniformity of the substrate, cells can spread equally and a directional movement to stiffer regions is clearly observed. Varying the geometry underlying the membrane, cell patterning and movement can be quantitatively characterized. This procedure is capable of controlling cell motility with high fidelity over large substrate areas. The most significant advance embodied in this method is that it offers the use of mechanical features to control cell adhesion and not topographical or chemical variations, which has not been reported so far. This modulation of the response of cell motility will be useful for the design and fabrication of advanced planar and 3D biological assemblies suitable for applications in the field of biotechnology and for tissue-engineering purposes.

1. Introduction

The control of the cell environment by multiple physicochemical cues is crucial to enable functionality, modulate response, and affect cell behavior. Over the past decade, a lot of attention has been focused on cell motility primarily because of the importance of the mechanical interactions of cells with the substrate. This can affect migration patterns,[1] cell differentiation, morphogenesis of tissues and organs,[2] wound healing and inflammation,[3] and cancer metastasis.[4,5] Cell motility also plays an important role in the realization of functional biomaterials, which will open up new insights for tissue engineering.[6] Efforts to understand the behavior of cells in response to interactions with their environment have been made by several researchers, which have investigated the potential of controlling cell movement by tuning the surface chemistry, topography, or substrate mechanics. This can be based on variations of either gradients of soluble or surface-attached chemicals (chemotaxis and haptotaxis, respectively),[7–10] light intensity (phototaxis),[11] extracellular tension (tensotaxis),[12] electrostatic potential (galvanotaxis),[13] and gravitational potential (geotaxis),[14] or focused on the rigidity of the substrate (mechanotaxis or durotaxis).[15] So far mechanical forces and the physical environment surrounding the cells have been shown to be a key factor for the cell's response, via active mechanosensing processes at cell–matrix adhesions, resulting in the formation of actin-rich organelles termed lamellipodia and filopodia.[16] Reports have shown the influence of mechanical interactions on cells through morphological and functional modifications, revealing how cells respond to the elastic properties of their environment by changing the substrate elasticity, varying chemical properties,[17–19] the thickness, or uniformity of the substrate. All of these reports, however, used surfaces with limitations due to physical and chemical changes, covering only a limited number of aspects that are significant for the understanding of the mechanisms responsible for the cells' interaction. Thus, the design of a substrate that can control directional movement of cells while maintaining constant physical and chemical properties to avoid undesirable responses is a significant challenge. In this work, we investigate cell migration by varying the mechanical rigidity of the substrate through the use of polydimethylsiloxane (PDMS) with precise control of movement and spatial arrangement on the substrate, a technique known as mechanotaxis. PDMS is a material widely used in biomedical applications[20] and in membrane technology[14] for its biocompatibility,[21,22] mechanical compliance, chemical inertness, and remarkable flexibility.[23] Because of the simplicity in tuning the elasticity (the elasticity modulus is directly related to the stiffness)[24–27] and cell behavior,[28,29] PDMS is particularly suitable for prototyping substrates for mechanotaxis means. The technique presented herein is an innovative straightforward method to micropattern and control cell movement on uniform PDMS substrates and will be useful for a number of biological

[*] B. Cortese, Prof. G. Gigli
National Nanotechnology Laboratory (NNL) of CNR-INFM
Distretto Tecnologico ISUFI
Engineering of Innovation Department
Lecce University
Via Arnesano Km 5, 73100 Lecce (Italy)
E-mail: barbara.cortese@unile.it
Prof. M. Riehle
Centre for Cell Engineering
Institute of Biomedical and Life Sciences
University of Glasgow
Glasgow, G12 8QQ (UK)

DOI: 10.1002/adfm.200900918

processes particularly in tissue engineering. This method introduces a new approach in studying mechanotaxis and allows control of cell motility and organization independently from topography limitations as an identical surface is displayed with respect to the cells. In fact the difference in gradient rigidity is related to the pattern underneath the membrane. Our approach involves, essentially, the fabrication of a 50:1 (w/w) soft membrane used to top a stiffer substrate, of which, to our knowledge, there are no previous studies because of the difficulty in handling such thin and elastic membranes. These membranes served as uniform substrates to enable the sensitivity of cell motility and focal adhesions based on substrate flexibility[25,26] and development of a directional movement of the cells. In particular, by varying the geometry of the pattern underneath, we have also developed a simple way of cell patterning and controlling cell movement. We illustrate this approach by patterning different types of cells (NIH 3T3, hTERT fibroblasts and C2C12, myogenic cells) in different geometric patterns. Different cells were chosen to investigate how these substrates influence proliferation and motility. The concurrent homogeneity of both the surface chemistry and topography opens up possibilities to vary the mechanical rigidity maintaining an identical environment, allowing cells to spread uniformly on the surface, and to respond only through active tactile exploration.[14] The response of cells to surfaces was evaluated by live microscopy and systematically investigated by immunostaining.

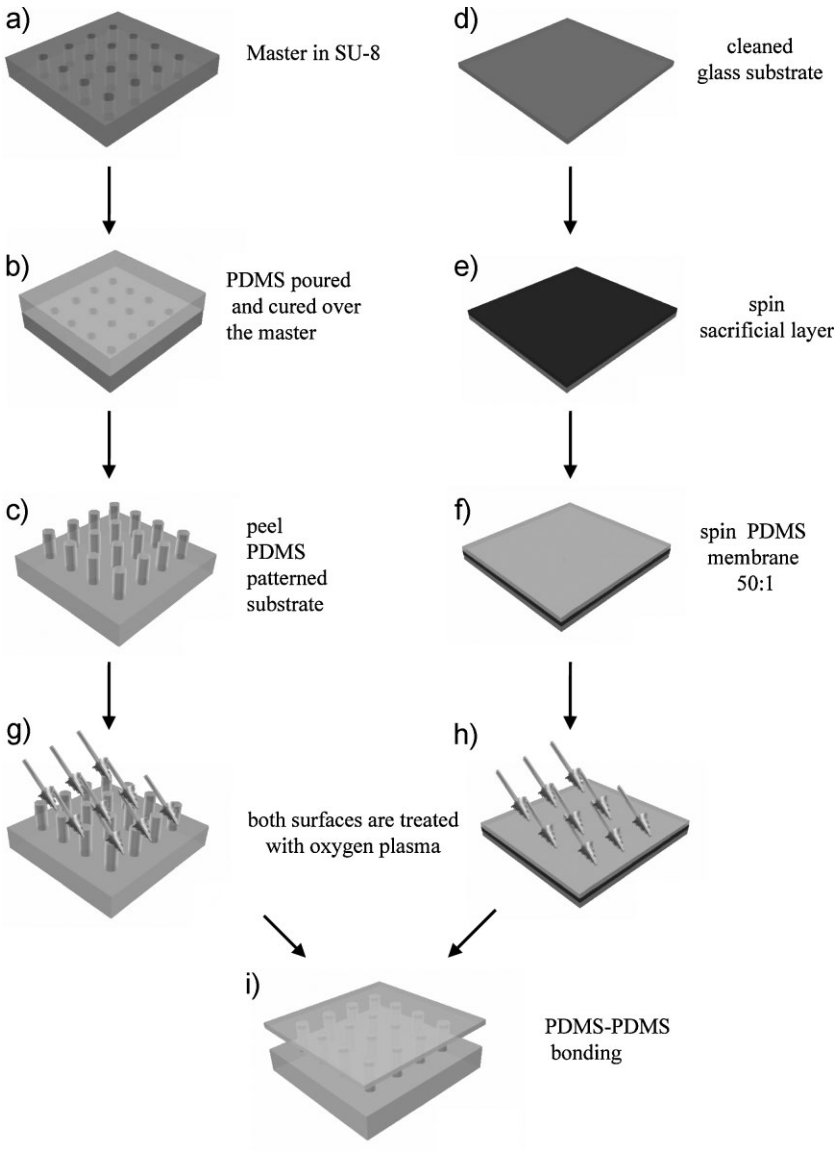

Figure 1. Steps of the fabrication process of the thin membrane on the substrate. a–c) The PDMS substrate was created by pouring a pre-polymer of PDMS on a pre-patterned SU8 substrate (a), which was cured at 80 °C for 1 h and subsequently peeled off (b,c). d–f) Thin membranes were fabricated by pouring a layer of trehalose on a glass cover slip (d,e) and spin coating a thin membrane of PDMS (f). g,h) Oxygen plasma treatment for PDMS bonding of substrate and membrane, as indicated by the arrows, was then performed on both, and i) after trehalose release, the final substrate with membrane was obtained.

2. Results and Discussion

2.1. Fabrication of 2D Topographically Patterned Uniform Substrates

Poly(dimethylsiloxane) (PDMS) stamps with embedded patterns of various geometrical shapes and sizes were fabricated by simply replicating a master patterned previously by photolithography[30] (Fig. 1). Patterns were either square or round pillars, grooves and ridges or pillars of different shapes and sizes placed in pits, as schematically shown in Figure 2. The characteristic feature sizes were as follows: the width for pillars and grooves ranged from 5–60 μm and the height was about 25 μm. The membrane was prepared through dilution with heptane, steps d to f (Fig. 1), and subsequently spin coated on a thin sacrificial layer. The thickness of the thin PDMS membrane was easily controlled by optimizing the dilution ratio, and spin coating time and speed in order to obtain a thickness of about 6 μm (see Experimental Section). The patterned PDMS substrates and membrane were subsequently exposed to an oxygen plasma and brought into contact to obtain an irreversible PDMS–PDMS bonding. The membrane was freed by dissolving the sacrificial layer resulting in the final assembly of a thin soft PDMS membrane bonded on top of a harder patterned PDMS substrate (step i) (Fig. 1). After release of the sacrificial layer the surfaces were thoroughly washed alternately with sterilized water and ethanol, after which they were coated with fibronectin before seeding of cells. The addition of fibronectin was necessary to facilitate cell attachment, because of the hydrophobicity of PDMS, and to improve the bioactivity of the surface.[31–33] A variety of patterned

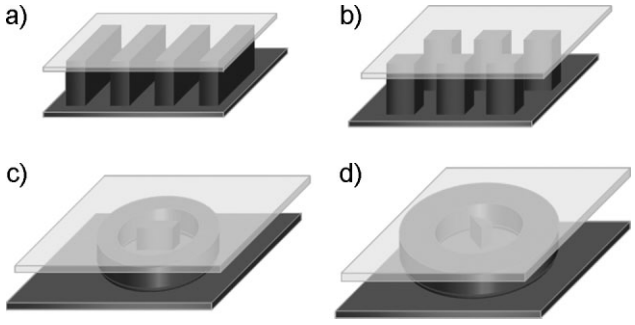

Figure 2. Schematic of the constructions made of a membrane bonded to underlying patterns with different geometries, ranging from a) lines, b) pillars, to c,d) various shapes of pillars, such as rectangles and triangles, placed in pits.

substrates with different geometries were made with an identical membrane on top of each pattern in order to investigate the role that substrate rigidity plays in controlling cell movement. The regions with patterned structures underneath the membrane were the stiff regions whereas those with only air underneath were the soft regions. The concentration of the mixing ratio of PDMS/curing agent of the membrane as well as the height was crucial to the effectiveness of the method. The thickness and elasticity of the membrane influenced the cell's interaction with the mechanical stimuli of the environment, and qualitatively different behaviors were observed. The cell function, including the morphology and orientation of adherent cells, improved significantly with the diminution of the Young's modulus (E). Hard membranes (with a mixing ratio of 10:1, $E = 306 \pm 10$ kPa[18–34]) caused poor adhesion of cells, and they were too thick for mechanical stimuli to influence the substrate response of the cells. In these regimes, cells spread uniformly without signs of recognizing the differences between stiff or soft regions (Fig. 3). The elastic modulus of the membrane was therefore decreased to 21.6 ± 3 kPa, as the ratio of PDMS elastomer base to cross linker was increased from 10:1 to 50:1, (Fig. S1 in the Supporting Information). More striking was the influence of heptane which plays a determining role in decreasing the Young's modulus with a sensitive reflection of the cellular response and it enhances the 'preference' for stiffer regions. Experimental results (see Fig. S2 in the Supporting Information) showed a further decrease of the elastic modulus to 0.76 ± 0.07 kPa, thus improving the control of cell motility. In fact, on the softest membranes (760 Pa), cells adhered and migrated for the duration of the whole experiment. Optical and scanning electron microscopy (SEM) images (Fig. 4) confirmed a flat uniform surface with underlying patterns, without the need for topographical cues to influence cell actions.

2.2. Analysis and Time-Lapse Quantification of Cell Migration

Time-lapse observations at high magnification were provided to verify the influence of the rigidity gradient on the cell's growth and

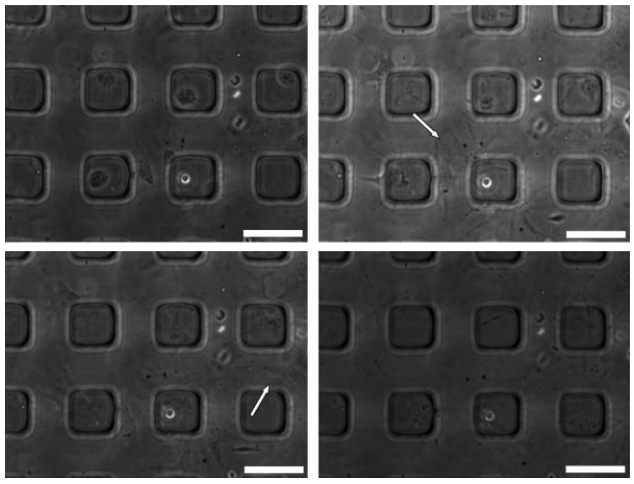

Figure 3. Time-lapse observation of a thin 10:1 PDMS membrane on top of a pillar-patterned surface. The cells can be seen to move on top of the membrane without any sign of recognizing the mechanical differences within the environment, spreading widely around without being constrained on the patterns, as highlighted by the white arrows. Cells are on top of both the stiff and soft regions. These images were obtained from approximately 1 h after seeding the cells on the substrate, with intervals of 60 min. Scale bar: 50 μm.

movement in response to the underlying patterns. The patterned substrates were placed in 60 mm plate wells and immersed in the culture media. NIH 3T3 (mouse embryonic fibroblast cell line) fibroblasts were evenly plated across the surfaces and kept alive and healthy during the observation time by encapsulating the samples in small homemade chambers where the temperature, humidity, and CO_2 atmosphere (5%) were maintained constant. Migration was recorded over 24 h, and the images of the cell distribution were quantified using Image J. We observed that cells adhered evenly as no physical barrier was introduced. At 1 hour after seeding, cells were attached and spread across the surface, thus, being able to probe the surface and move freely on both the soft and stiffer regions (Fig. 5a). The lamellipodia and filopodia filaments oriented themselves randomly as the cells explored the environment

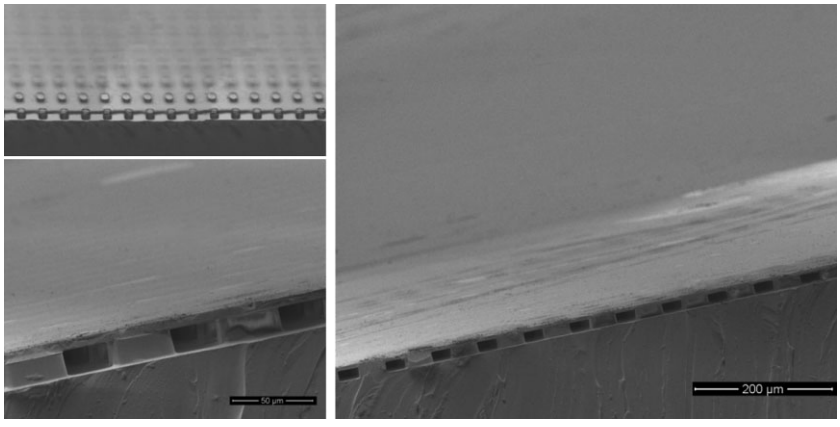

Figure 4. Optical and SEM microscopy images of the suspended thin (ca. 6 μm) 50:1 PDMS membrane on top of a pillar-patterned surface. The uniformity of the membrane above the underlying pattern is clearly shown.

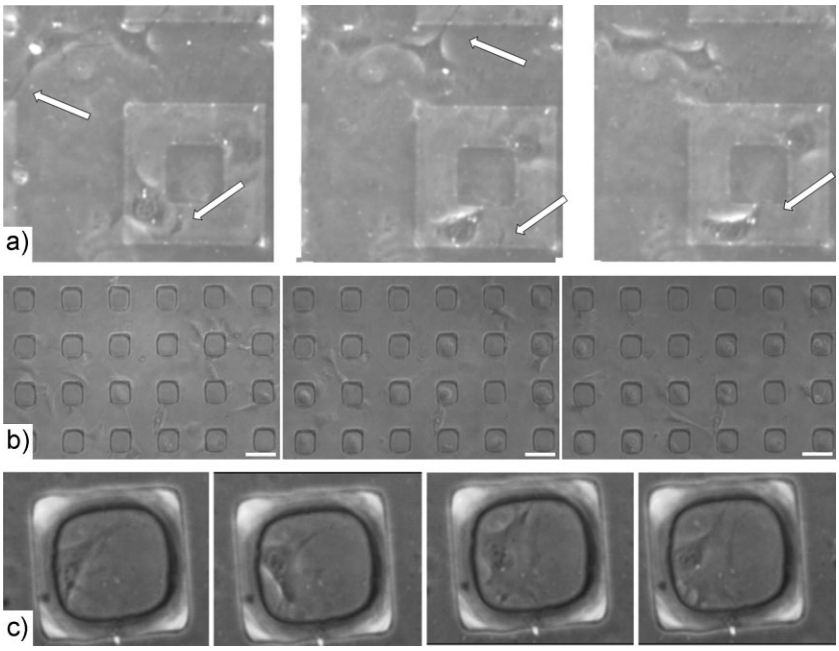

Figure 5. Different sequences of time-lapse microscopy images of NIH 3T3 cells moving on the membrane, on top of square pillars in pits (a) and square pillar-patterned substrates (b,c). The stiff regions are represented by the squares while the soft regions are the surrounding areas. In these images the cells initially move around freely but once they feel the mechanical cues of the environment they clearly start moving away from the soft regions (a) or by moving on top of the squares (which are the stiffer regions) (b). In the last sequence (c) a magnification of a single cell moving in a confined manner on a square pillar, probing the ridges of the pattern is shown. All images were obtained from approximately 1 h after seeding cells on the substrate, and the interval between each image was about 30 min. Scale bar: 50 μm.

probing the different mechanical initial positions, and remained confined on the surface of the stiffer patterns detecting the mechanical gradient (Fig. 5). Analysis of our results indicated that cells on softer substrates move around more on the substrate than cells on stiffer substrates.[35–37] In fact on the soft regions of the substrates cells seemed to be highly motile, forming dynamic filopodia-like extensions while probing the substrate. Also, sensing the rigidity induced by the pillars, cells reoriented themselves while moving along the ridges of the stiff pattern (Fig. 5c), showing a preferential accumulation on stiffer regions, and an avoidance of staying too long on soft substrates.[38,39] Even in the presence of cell–cell contacts, the cells simply reoriented themselves in the direction of the stiffer regions (Fig. 6), moving in such a way as to maximize the mechanical input from the substrate, or shifting towards the nearest stiffer patterns. A net accumulation on stiffer regions became more evident after 24 h after being seeded.

To investigate the dynamic behavior of cells[40,41] we observed cell proliferation of C2C12 mouse myoblast cell line, myogenic cells on line-patterned substrates by means of phase-contrast microscopy. Quantitative analysis of the alignment of the cells revealed the strong influence of the underlying pattern on cellular alignment. Cell migrations guided along stiff lines were observed as the C2C12 myotubes followed and aligned along the preferential direction of the darker lines, which are the stiff regions, showing how the extension of cell protrusion and their adhesion are linked to the substrate's underlying pattern. Nuclear alignment angles were determined by using Image J, counting cells with alignment angles of less than 10° as aligned. As expected, cells on membranes with no pattern underneath exhibited a uniform distribution of alignment angles.[42] Cells on a suspended membrane bonded to a micro-grooved substrate were found to exhibit similar orientations corresponding to the groove direction with a peak percentage of $88 \pm 5\%$, while cells on pillar-patterned substrates were found to be oriented at angles of approximately 45° and −45° with respect to an arbitrary direction horizontal to the square pillar pattern (Fig. 7). Morphological changes related to the substrate underlying pattern were confirmed by SEM analysis (Fig. 8), showing the alignment of the cells along the line-patterned substrate despite the presence of the membrane. SEM analysis revealed that cell–substrate contacts were restricted to the tops of the ridges of the stiff patterns, regardless of a uniform surface. To ultimately better characterize migration, the distribution of the average cell speed was analyzed as shown (Fig. 9). The average speed of cells cultured on soft substrates was significantly higher than those cultured on flat control substrates.[43] Cells cultured on membranes with underlying pillar-patterned substrates exhibited similar speeds, and migration speeds were significantly higher before cells moved on top of the pillars. After reaching the stiffer region, the mean value of the cell speed remained mainly constant, as cells moved only inside the ridge of the pattern. Rapid migration was therefore observed on soft substrates rather than stiffer ones, as cells used the edge of the stiff patterns as a grip,

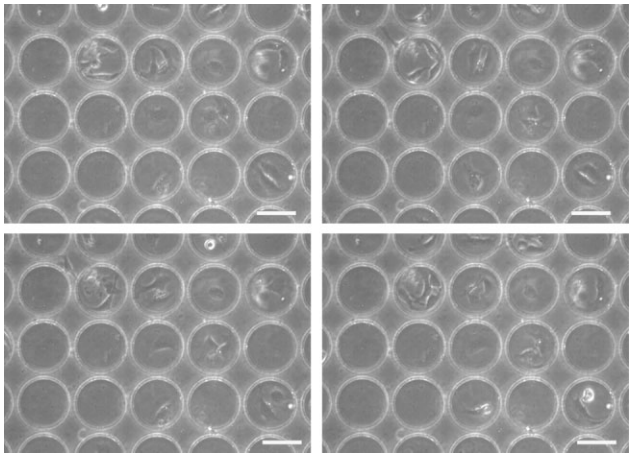

Figure 6. Time-lapse microscopy images of NIH 3T3 cells moving on the membrane, with a round-pillar pattern underneath. In these images cells are clearly filling in on the circular pillars. Images were obtained from approximately 1 h after seeding the cells on the substrate, and the interval between images was about 60 min. Scale bar: 50 μm.

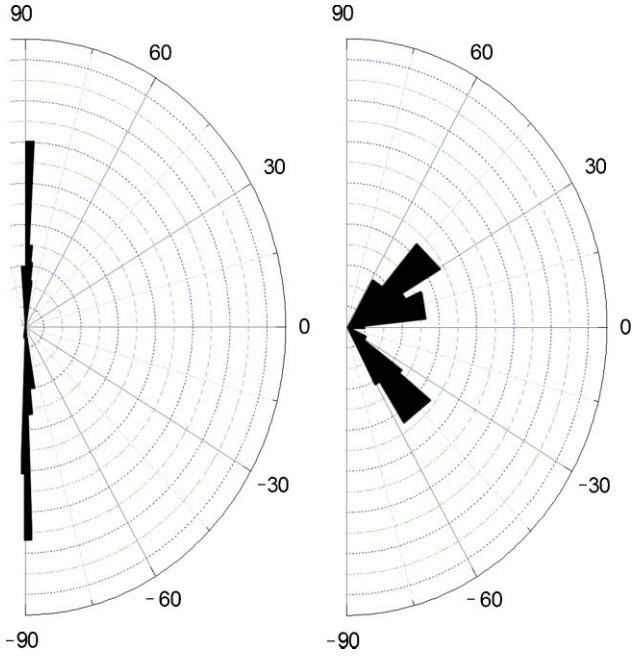

Figure 7. Cell angular distribution on the membrane suspended on lines on the left, and pillars, on the right. The cells showed a high degree of alignment ($n = 100$ for each group). The measurement of 90° indicates perfect alignment with the grooved pattern.

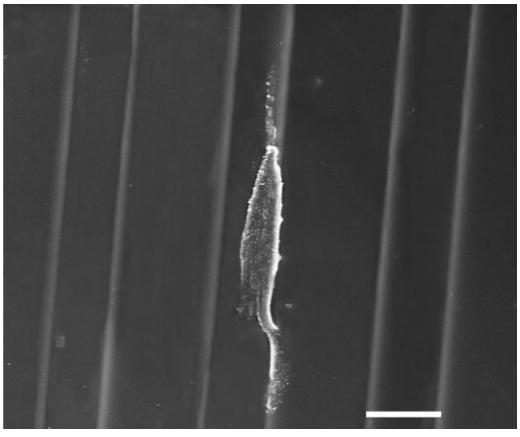

Figure 8. SEM image representing the orientation and morphology of cells on a membrane with an underlying groove patterned surface. The lines are 20 μm and the distance between lines is 30 μm. The cell clearly aligns to the underlying substrate. Scale bar: 20 μm.

clinging on the border lines for mechanical movement.[44] In order to focus on the movement of the cells themselves, a sequence of phase-contrast images were obtained at six different time points (after 1h of seeding followed by intervals of 30 min) showing a rapid parallel orientation of the lines, and fast movement of the cells along the orientation direction, as indicated by the white arrow (Fig. 10). The figure clearly shows that cells migrated on the ridges of the lines, which was restricted because of the interval of the grooves. Interestingly, the migration rate on the line-patterned surface seemed to be larger than that of pillar-patterned surfaces,

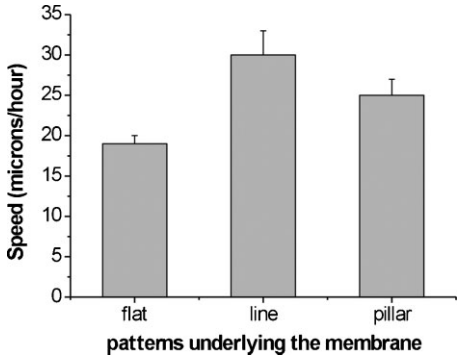

Figure 9. Plot of time-lapse microscopy data of the average speed (μm h^{-1}) recorded following a single cell over 24 h ($n = 6$).

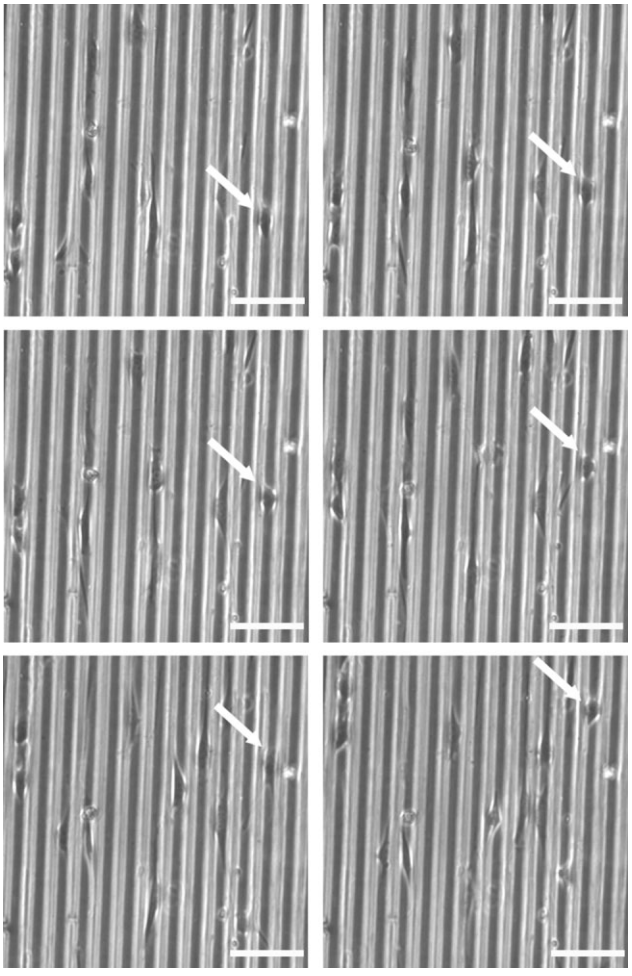

Figure 10. Time-lapse phase-contrast images of human fibroblast cells moving on the membrane. The darker lines are the patterned grooves underneath the membrane. In this sequence of images, cells feel and respond to the substrate clearly moving along the ridges of the lines on the harder regions. Attention has been focused on a particular cell moving rapidly towards the top (indicated by white arrows). Images were obtained from approximately 1 h after seeding the cells on the substrate, and the interval between images was about 30 min. Scale bar: 100 μm.

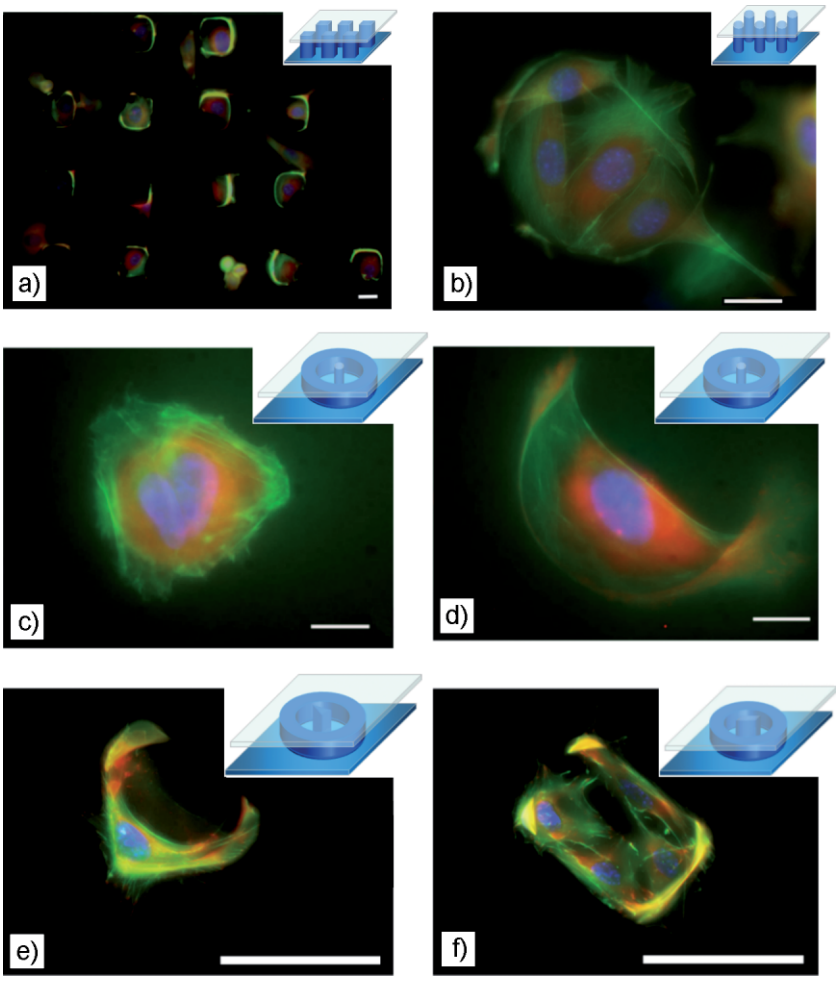

Figure 11. Fluorescent images of NIH 3T3, cultured for 24 h, stained for vinculin in green, plated on square-patterned substrates and pillars in pits for 24 h. DNA is blue and actin is red. The figures outline the stiff regions, caused by the presence of the patterns underneath the membrane, outlined in the insets, whereas the regions surrounding the pillars are soft. Different geometries of the underlying patterns were used: a) square pillars; b) round pillars, c,d) round pillars placed in pits, e) triangular, and f) rectangular pillars placed in pits. In the latter the cells tend to migrate on the stiffer regions placed in the middle of the pit, sensing the ridges, which induces the patterned effect. Scale bars: 20 μm.

suggesting that the geometry of the underlying patterns, as well as the stiffness, is a critical parameter in cell motility speed.

Immunostaining was used to observe cellular attachment, spreading, and distribution of the cells' cytoskeletons. The fluorescence images reported (Fig. 11) showed the formation of adhesive contacts during cell spreading and indicated that the actin filaments and focal adhesions oriented themselves according to the stiff pattern underneath the membrane, confirming the ease of controlling the cell positioning. It is clearly shown that cells, despite the presence of a membrane, sensed the ridges of the pattern underneath, shown in the insets of the figure, thereby, covering only the stiffer regions, which induced a subsequent patterning of the surface. As is evident from the figure, the formation of filopodia and lamellipodia occurred mostly around the edges of the stiff underlying patterns. The latter, therefore, highlights the presence of a rigidity gradient, and a correlation between the responsive mechanism of the cell motility and the matrix rigidity. As a result the cell adhesion and the formation of focal contacts are affected by this. Furthermore, to observe how geometric features influenced cell adhesion and spreading, pillars of different shapes and geometries were placed in pits and subsequently covered with a membrane (Fig. 11c–e). These particular geometries evidence the fact that cells have a stretched and organized actin cytoskeleton on the stiff substrates, demonstrating articulated stress fibers as cells reach over the soft parts to get to the stiff regions (Fig. 11c,d). Cells were localized not only on the surrounding stiff regions but also on central stiff areas of the pits, assuming the shape of the underlying pattern (Fig. 11d,e).

The fact that cell motility can be controlled by patterns, solely by a preference for stiffer regions as no other physical or chemical changes had been introduced during cell migration, suggests a new method to control cells' movement in uniform environments. The common observation made from these experiments is that the substrate rigidity does play a crucial role in the cell motility, inducing a patterning of the cells on the surface.

The role of rigidity on spreading was further characterized by quantifying the cell distribution on the different substrates. Cells were counted 24 h after cell seeding, and the spread area of individual cells was quantified using Image J software. The ratios of the number of cells on the stiff and soft regions to the number on the whole area were counted for each pattern, and plotted (Fig. 12), showing a preferential accumulation of cells on the stiff regions of patterned substrates. From these results, we can see how the distribution of cells is influenced by the gradient stiffness of the pattern underneath.

3. Conclusions

Planar and controlled patterned surfaces can be fabricated in a simple and versatile way, allowing through experiments of this kind to examine the migratory behavior of the cells on uniform substrates and the influence on cell motility. Although several methods for mechanotaxis have been explored before,[15,35–50] the major disadvantage of all these methods, compared to the method reported herein, is that they do not use a uniform environment with a well-defined geometry. We have found several advantages using this assembly, which enabled patterning of cells on the surface of the PDMS membrane and thus render the method suitable for applications in the biotechnology field. Our method is in fact simple to implement and it confines cells to specific areas while at the same time allows us to study mutual interactions of

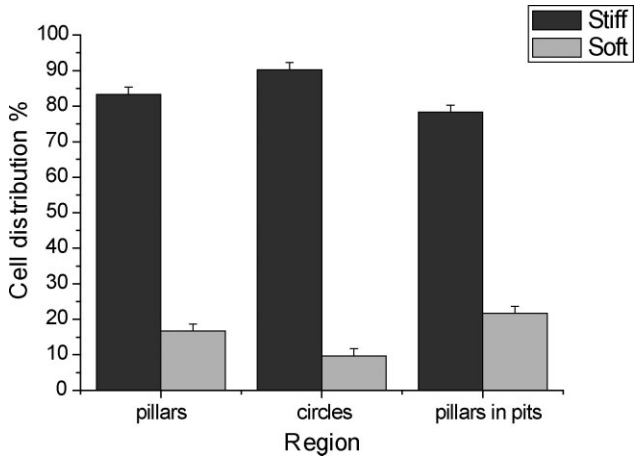

Figure 12. Plot of the total cell density after 24 h of incubation on the structures. The percentage of cells remaining on the substrate shows a significant difference between stiff or soft regions, namely, it is much higher on the stiff regions. The error bars represent standard deviations.

cells through the liquid medium surrounding them. On the other hand, mechanical patterning provides an alternative to chemical patterning[39,40] and as both methods can be controlled independently from each other new ways of patterning can be achieved. The comprehension of the physical characteristics is relevant in understanding how migratory processes of cells are regulated by mechanical forces, which is important for processes such as mechano-transduction, embryological development, and wound healing. Our results demonstrate that substrate stiffness has a profound effect on the response of cells, because of the rigidity gradient of the substrate, which was evidenced by the accumulation of cells in stiff areas versus soft areas, suggesting that mechanotaxis alone was responsible for the observed accumulation. We believe that our planar PDMS substrates with tunable stiffness rigidity will be useful to investigate and exploit cell behavior without being confined to particular substrate geometries or having to invest in complex fabrication tools. Further studies will be made to define the mechanism of cell movement in response to substrate rigidity and will be focused on the investigation and understanding of mechano-transduction and the role of focal adhesion.[42,43] Our innovative approach suggests potential applications for studies of the mechanism of cell migration by a rigidity gradient, for biomedical and tissue-engineering purposes.

4. Experimental

Substrate Preparation and Characterization: Polydimethylsiloxane (PDMS) composed of an elastomer base and a curing agent [51], was purchased from Dow Corning (Midland, MI). A 10:1 mixture (w/w) of prepolymer and curing agent, was generally prepared and left to settle for 10 min in vacuum, so that the trapped air bubbles could emerge to the surface. After the removal of all the air bubbles, the mixture was poured on a SU8 (MicroChem Corp., USA) master realized with photolithography and subsequently placed in an oven (80 °C) for curing for 1 h, and subsequently samples were gently peeled from the mold [52].

The thin membrane was prepared from a 50:1 mixture (w/w), and diluted with heptane (Sigma Aldrich, UK) [53,54], with the purpose of reducing the Young's modulus, as elaborated in the Supporting Information. The mixture was gently poured on a cover glass slip (Menzel Gläser), previously cleaned, and coated with Trehalose (Sigma Aldrich, UK), and spun at 3000 rpm to obtain a thickness of 6 μm. After baking at 80 °C for 1 h, the membrane and substrates were both exposed to an oxygen plasma for 10 s in an Edwards glow discharge in air. Both samples were then placed together within a minute of the glow discharge to obtain irreversible bonding. The resulting substrate was, subsequently, easily peeled off from the Trehalose-coated cover slip.

The Young's modulus (E) of the substrate was determined using a tensile test method described previously [18]. Briefly, PDMS sheets (50 mm × 20 mm × 0.5 mm) were stretched in response to known applied forces. A plot of strain (F/A) versus stress ($\Delta L/L$), where F is the force, A is the cross-sectional area, L is the original length and ΔL is the change in length, was measured. Measurements showed a significant decrease between membranes diluted with heptane and those without.

Cell Culture: Infinity telomerase immortalized human fibroblasts (hTERT-BJ1, Clonetech Laboratories, Inc., USA), National Institute of health 3T3 (NIH 3T3) (ATCC, Rockville, MD), and C2C12 muscle precursor cells (murine myoblast cell line, CRL-1772, ATCC, Rockville, MD, USA) were maintained in Dulbecco's-modified Eagle's medium (DMEM, Invitrogen, Carlsbad, CA) supplemented with 10% calf serum (FCS) (Life Technologies, UK), 1.6% 200 mM L-glutamine, and 0.9% 100mM sodium pyruvate (Life Technologies, UK) at 37 °C in a 5% CO_2 humidified incubator. After reaching confluence cells were detached and seeded onto the substrates at a density of 5×10^4 cells per sample.

Immunofluorescence: Cells were fixed in 4% formaldehyde (Sigma Aldrich, UK)/ phosphate buffered saline (PBS) (Invitrogen, CA), with 1% sucrose at 37 °C for 15 min. After rendering permeable with 5% Triton X-100 (Sigma Aldrich, UK) in PBS, and blocking with 1% bovine serum albumin (BSA) (Sigma) in PBS (Invitrogen), cells were incubated in mouse antibody vinculin (Sigma Aldrich, UK) and phalloidin (Invitrogen) at 37 °C, followed by 1 h of incubation with biotinylated anti-mouse IgG (H + L) secondary antibody (Vector Laboratories). Subsequently, cells were stained with a third antibody, Texas Red streptavidin (Vector Laboratories). Each antibody was diluted at 50:1, in a BSA solution in PBS. The samples were rinsed three times for 5 min in 0.5% Tween 20 (Biochemical BDH Laboratory Supplies)/PBS between each staining. The surfaces were mounted using Vectashield DAPI (Vector Laboratories) and then viewed by fluorescence microscopy (Zeiss Axiovert 200M).

Time-Lapse Video Recordings: Samples were seeded in single 60 mm tissue-culture plates, and sealed in small chambers with controlled temperature, humidity, and CO_2 concentration. Cell division was monitored using a Zeiss Axiovert 25 inverted microscope equipped with a CV-M50 (Alrad Instruments, Newbury UK) digital camera and controlled by Time Warp Advision software (Alrad Imaging, www.alrad.com). For determination of cell motility, images stored sequentially with an interval between observations of 1 min, for a total observation time of 24 h, were subsequently mounted and analyzed using Image J analysis software (Image J, http://rsb.info.nih.gov/ij).

Quantification of Cells: Samples fixed in 4% formaldehyde/PBS were then stained for 20 min in 0.5%. Coomassie blue (Biochemical BDH Laboratory Supplies) in a methanol/acetic acid aqueous solution, and washed with PBS. Samples were then observed by an inverted light microscopy with a 10× objective (Zeiss Axiovert 25) and analyzed with image analysis. Cell orientation angles were quantified using ImageJ, determining the angle with respect to the parallel direction of the groove and the direction of the longer axis of the approximated ellipse of the nucleus, which approximates the cell shape, whereas on smooth control surfaces a random orientation was observed. In the case of different patterned samples, orientation was measured with respect to an arbitrary direction.

Acknowledgements

The authors thank Stefania D'Amone for useful technical support. Antonio Qualtieri is gratefully acknowledged for the SEM images. We thank Nikolaj

Gadegaard for master supports. We also thank Lina Altomare for seeding of the C2C12 cells. Technical assistance from Anne McIntosh, Margaret Mullin, and Andy Hart is gratefully acknowledged. We also acknowledge funding from Scuola Superiore Isufi-Universitá del Salento. Supporting information is available online from Wiley InterScience or from the author.

Received: May 27, 2009
Published online: July 24, 2009

[1] N. Wang, E. Ostuni, G. M. Whitesides, D. E. Ingber, *Cell Motil. Cytoskeleton* **2002**, *52*, 2.
[2] R. L. Juliano, S. Haskill, *J. Cell Biol.* **1993**, *120*, 3.
[3] P. Martin, *Science* **1997**, *276*, 75.
[4] L. R. Bernstein, L. A. Liotta, *Curr. Opin. Oncol.* **1994**, *6*, 1.
[5] D. E. Ingber, D. Prusty, Z. Sun, H. Betensky, N. Wang, *J. Biomech.* **1995**, *28*, 12.
[6] A. Curtis, M. O. Riehle, *Phys. Med. Biol.* **2001**, 46.
[7] S. B. Carter, *Nature* **1965**, *208*, 16.
[8] N. L. Jeon, H. Baskaran, S. K. W. Dertinger, G. M. Whitesides, L. Van De Water, M. Toner, *Nat. Biotechnol.* **2002**, *2*, 826.
[9] L. Helmick, A. A. de Mayolo, Y. Zhang, C. M. Cheng, S. C. Watkins, C. Wu, P. R. LeDuc, *Nano Lett.* **2008**, *8*, 1303.
[10] D. Bray, *Cell Movements: From Molecules to Motility*, 2nd ed., Garland Publishing, New York, NJ **2001**.
[11] J. Saranak, K. W. Foster, *Nature* **1997**, *387*, 465.
[12] L. V. Beloussov, N. N. Louchinskaia, A. A. Stein, *Dev. Genes. Evol.* **2000**, *210*, 2.
[13] C. A. Erickson, R. Nuccitelli, *J. Cell Biol.* **1984**, *98*, 1.
[14] C. F. Adams, A. J. Paul, *J. Crustacean Biol.* **1999**, *19*, 1.
[15] C. M. Lo, H. B. Wang, M. Dembo, Y. L. Wang, *Biophys. J.* **2000**, *79*, 1.
[16] U. S. Schwarz, I. B. Bischofs, *Med. Eng. Phys.* **2005**, *27*, 9.
[17] R. J. Pelham, Y. L. Wang, *Proc. Natl. Acad. Sci. USA* **1997**, *94*, 25.
[18] D. S. Gray, J. Tien, C. S. Chen, *J. Biomed. Mater. Res. A* **2003**, *66*, 3.
[19] P. Kuntanawat, C. Wilkinson, M. O. Riehle, *Comp. Biochem. Phys. Part A: Molec. Integr. Physiol.* **2007**, *146*(4), S192.
[20] J. C. McDonald, G. M. Whitesides, *Acc. Chem. Res.* **2002**, *35*, 7.
[21] Y. Zhao, C. C. Lim, D. B. Sawyer, R. Liao, X. Zhang, *J. Micromech. Microeng.* **2005**, *15*, 9.
[22] A. Gadre, M. Kastantin, S. Li, R. Ghodssi, *Proc. Int. Semiconductor Device Research Symp.*, Washington DC, **2001** p.p. 186–189.
[23] *Membrane Technology* (Eds: S. P. Nunes, K.-V. Peinemann), Wiley-VCH, Weinheim, Germany **2001**.
[24] F. Carrillo, S. Gupta, M. Balooch, S. J. Marshall, G. W. Marshall, L. Pruitt, C. M. Puttlitz, *J. Mater. Res.* **2005**, *20*, 10.
[25] A. Engler, L. Bacakova, C. Newman, A. Hategan, M. Griffin, D. Discher, (journal?) **2004**, *86*, 2.
[26] T. Yeung, P. C. Georges, L. A. Flanagan, B. Marg, M. Ortiz, M. Funaki, N. Zahir, W. Ming, V. Weaver, P. A. Janmey, *Cell Motil. Cytoskel.* **2005**, *60*, 1.
[27] J. E. Puskas, Y. Chen, *Biomacromolecules* **2004**, *5*, 4.
[28] J. C. Lötters, W. Olthuis, P. H. Veltink, P. Bergveld, *J. Micromech. Microeng.* **1997**, *7*, 3.
[29] X. Q. Brown, K. Ookawa, J. Y. Wong, *Biomaterials* **2005**, *26*, 16.
[30] B. Cortese, S. D'Amone, M. Manca, I. Viola, R. Cingolani, G. Gigli, *Langmuir* **2008**, *24*, 6.
[31] G. K. Toworfe, R. J. Composto, C. S. Adams, I. M. Shapiro, P. Ducheyne, *J. Biomed. Mater. Res. A* **2004**, *71*, 449.
[32] T. Y. Chang, V. G. Yadav, S. De Leo, A. Mohedas, B. Rajalingam, C. L. Chen, S. Selvarasah, M. R. Dokmeci, A. Khademhosseini, *Langmuir* **2007**, *23*, 11718.
[33] a) P. J. Wipff, H. Majd, C. Acharya, L. Buscemi, J. J. Meister, B. Hinz, *Biomaterials* **2009**, *30*, 1781. b) J. S. Burmeister, J. D. Vrany, W. M. Reichert, G. A. Truskey, *J. Biomed. Mater. Res.* **1996**, *30*, 13.
[34] D. Fuard, T. Tzvetkova-Chevolleau, S. Decossas, P. Tracqui, P. Schiavone, *Microelectron. Eng.* **2008**, *85*, 1289.
[35] W. Guo, M. T. Frey, N. A. Burnham, Y. Wang, *Biophys. J.* **2006**, *90*, 2213.
[36] A. Saez, M. Ghibaudo, A. Buguin, P. Silberzan, B. Ladoux, *PNAS* **2007**, *104*, 8281.
[37] G. Jiang, A. H. Huang, Y. Cai, M. Tanase, M. P. Sheetz, *Biophys. J.* **2006**, *90*, 1804.
[38] K. F. Ren, T. Crouzier, C. Roy, C. Picart, *Adv. Funct. Mater.* **2008**, *18*, 1378.
[39] N. Zaari, P. Rajagopalan, S. Kim, A. Engler, J. Wong, *Adv. Mater.* **2004**, *16*, 2133.
[40] J. Y. Wong, J. B. Leach, X. Q. Brown, *Surf. Sci.* **2004**, *570*, 119.
[41] S. Gupton, C. Waterman-Storer, *Cell* **2006**, *125*, 1361.
[42] D. H. Kim, C. H. Seo, K. Han, K. W. Kwon, A. Levchenko, K. Y. Suh, *Adv. Funct. Mater.* **2009**, *19*, 1.
[43] J. P. Kaiser, A. Reinmann, A. Bruinink, *Biomaterials* **2006**, *27*, 5230.
[44] C. C. Berry, G. Campbell, A. Spadaccino, M. Robertson, A. Curtis, *Biomaterials* **2004**, *25*, 26.
[45] C. M. Cesa, N. Kirchgeßner, D. Mayer, U. S. Schwarz, B. Hoffmann, R. Merkel, *Rev. Sci. Instr.* **2007**, *78*, 3.
[46] H. B. Wang, M. Dembo, Y. L. Wang, *Am. J. Physiol. Cell Physiol.* **2000**, *279*, C1345.
[47] R. S. Kane, S. Takayama, E. Ostuni, D. E. Ingber, G. M. Whitesides, *Biomaterials* **1999**, *20*, 23.
[48] S. N. Bhatia, M. L. Yarmush, M. Toner, *J. Biomed. Mater. Res.* **1997**, *34*, 2.
[49] D. E. Ingber, *Curr. Opin. Cell Biol.* **1991**, *3*, 5.
[50] B. Geiger, A. Bershadsky, *Curr. Opin. Cell Biol.* **2001**, *13*, 5.
[51] Sylgard 184 silicone elastomer, product data sheet, http://www.dowcorning.com/DataFiles/090007b28117a63f.pdf (last accessed April 2008).
[52] SU-8 2000 data sheet, http://www.microchem.com/products/pdf/SU-82000DataSheet2000_5thru2015Ver4.pdf (last accessed September 2008).
[53] M. He, J. S. Edgar, G. D. M. Jeffries, R. M. Lorenz, J. P. Shelby, D. T. Chiu, *Anal. Chem.* **2005**, *77*, 1539.
[54] H. Hillborg, J. F. Anknerc, U. W. Gedde, G. D. Smithd, H. K. Yasudae, K. Wikströma, *Polymer* **2000**, *41*, 18.